Available online at www.sciencedirect.com
SCIENCE DIRECT®
Diamond and Related Materials 12 (2003) 905–910
DIAMOND AND RELATED MATERIALS
www.elsevier.com/locate/diamond

Resonant Raman spectra of amorphous carbon nitrides: the G peak dispersion

A.C. Ferrari[a,*], S.E. Rodil[a,b], J. Robertson[a]

[a]*Department of Engineering, University of Cambridge, Cambridge, CB2 1PZ, UK*
[b]*Instituto de Investigaciones en Materiales, Universidad Autónoma de México, Coyoacan, D.F. 04510, Mexico*

Abstract

A general model is presented for the interpretation of the Raman spectra of amorphous carbon nitrides measured at any excitation energy. The Raman spectra can be explained in terms of an amorphous carbon based model, without need of extra peaks due to CN, NN or NH modes. We classify amorphous carbon nitride films in four classes, according to the corresponding N-free film: a-C:N, a-C:H:N, ta-C:H:N and ta-C:N. In all cases, a multi-wavelength Raman study allows a direct correlation of the Raman parameters with the N content, which is not generally possible for single wavelength excitation. The G peak dispersion emerges as a most informative parameter for Raman analysis. UV Raman enhances the sp^1 CN peak, which is usually too faint to be seen in visible excitation.

Keywords: Diamond-like carbon; Carbon nitride; Raman spectroscopy; Structure

1. Introduction

There have been extensive efforts to create C_3N_4 since the prediction of its high bulk modulus and hardness comparable to diamond [1]. Most of the experiments actually produce amorphous carbon nitrides (a-C:N), which are of interest in their own right [2]. It is therefore important to be able to determine the bonding in carbon nitrides, especially by non-destructive techniques such as Raman spectroscopy. This paper provides an analysis of the Raman spectra of the various forms of carbon nitride films measured at various excitation wavelengths. In particular we will focus our attention on the study of the variation of position of the G peak with changing excitation energy: the G peak dispersion.

To do this, we classify carbon nitrides into four types: (a) the mainly sp^2 bonded a-C:N produced by sputtering, (b) the mainly sp^3 bonded ta-C:N produced by cathodic arc, pulsed laser deposition or mass selected ion beam deposition, (c) plasma deposited a-C:H:N with moderate sp^3 content, and (d) ta-C:H:N prepared by a high plasma density source, with a higher sp^3 content and lower hydrogen content.

The Raman spectra of carbon nitrides measured at any excitation energy have a similar form to those of N-free amorphous carbons. In this paper, we present a general model for their interpretation, extending our previous model for N-free carbon films [3,4] In this model, we noted that the Raman spectra depend fundamentally just on the configuration of sp^2 sites. An important factor is how the Raman spectra vary with photon excitation wavelength. Indeed, a main result of this paper is that a combination of visible and UV Raman gives a wealth of information on carbon nitrides, not available from a study at single wavelength. This makes resonant Raman scattering particularly useful for carbon nitrides. This contrasts with most previous Raman studies on carbon nitrides, which only used visible excitation [5–12], with only few recent works reporting UV Raman spectra of carbon nitrides [13–16]. Previous studies focused on finding signatures for C–N bonds, N=N bonds or N–H bonds in the Raman and IR spectra [17–20]. This paper adopts a different approach. The direct contribution of CN or NN or NH vibrations to the spectra will be neglected unless direct evidence of these is found.

*Corresponding author. Tel.: +44-122-376-4093; fax: +44-122-333-2662.
E-mail address: acf26@eng.cam.ac.uk (A.C. Ferrari).

0925-9635/03/$ - see front matter © 2003 Elsevier Science B.V. All rights reserved.
doi:10.1016/S0925-9635(02)00370-9

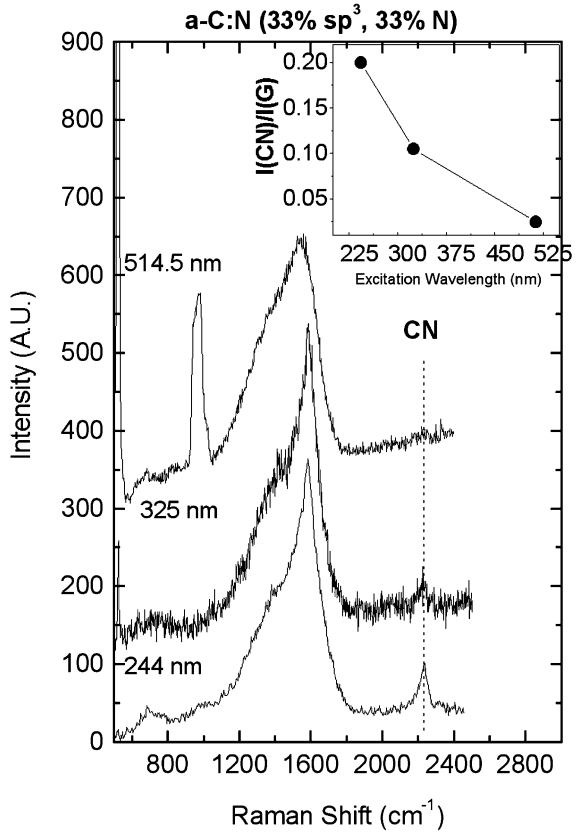

Fig. 1. Multi-wavelength Raman spectra of a 33% sp^3, 33% N a-C:N. For 514.5 nm and, to a lesser extent, 325 nm excitations the contributions of the substrate Si Raman peaks at ~521 and 970 cm^{-1} are also seen.

2. Raman spectra of carbon nitrides

The vibration frequencies of solid carbon nitrides are expected to lie close to the modes of the analogous unsaturated CN molecules, which are 1500–1600 cm^{-1} for chain-like molecules and 1300–1600 cm^{-1} for ring-like molecules [21,22]. This means that there is little distinction in the G–D region between modes due to C or N atoms. For example, the frequency of bond-stretching skeletal and ring modes is very similar in benzene, pyridine and pyrrole, so it is difficult to assess if an aromatic ring contains nitrogen or not. The modes in amorphous carbon nitrides are also delocalised over both carbon and nitrogen sites because of nitrogen's tendency to promote more clustered sp^2 bonding. We therefore expect little difference between the Raman spectra of nitrogenated and N-free carbon films in the 1000–2000 cm^{-1} region. Indeed, we found no shift in the Raman spectra of two sputtered CN samples, one with ~26 at.% ^{14}N and the other with the same content of ^{15}N.

The similarity of vibrational frequencies of C–C and C–N modes could make the interpretation of the skeletal modes quite difficult, if we were hoping to find C–N and N–N modes, as in some previous work [17–20]. However, we neglect the direct contributions of C–N or N–N bonds to the 1000–2000 cm^{-1} spectral range [5]. Instead, we analyse the trends in the G and D positions in the same way as in N-free samples. This will enable us to explain the observed spectra in the 1000–2000 cm^{-1} region, without needing to invoke heteropolar modes. On the other hand, UV Raman can detect CN sp^1 vibrations even when not seen in visible Raman, due to the resonant enhancement.

We consider each of the four classes of carbon nitrides. Fig. 1 shows the Raman spectra excited at 244, 325 and 514 nm of a a-C:N film with 33% N content and ~33% sp^3 bonding. The spectra were measured on a range of spectrometers and care was taken to avoid any damage, as previously described [3,4]. The spectra were then analysed by fitting a Lorentzian to the D peak and any T peak and a Breit–Wigner–Fano (BWF) lineshape to the G peak. The G peak position corresponds to the maximum of the BWF, rather than its centre [3].

Fig. 2a shows the variation of G peak position with N content, for 244 and 514 nm excitation. The G peak remains roughly constant with increasing N content for

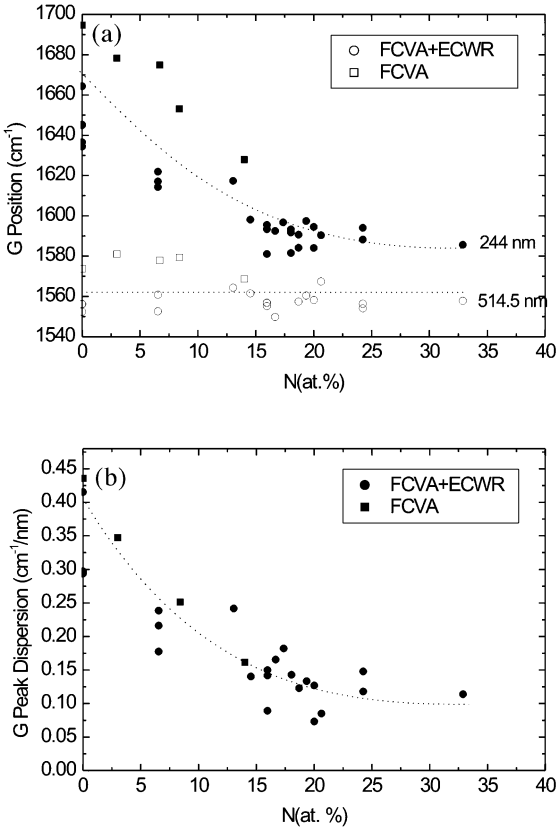

Fig. 2. (a) G peak position vs. N content for 244 and 514 nm excitation for (t)a-C:N samples deposited by FCVA+ECWR and FCVA alone. (b) dispersion of G peak vs. N content. The lines are guides to the eye.

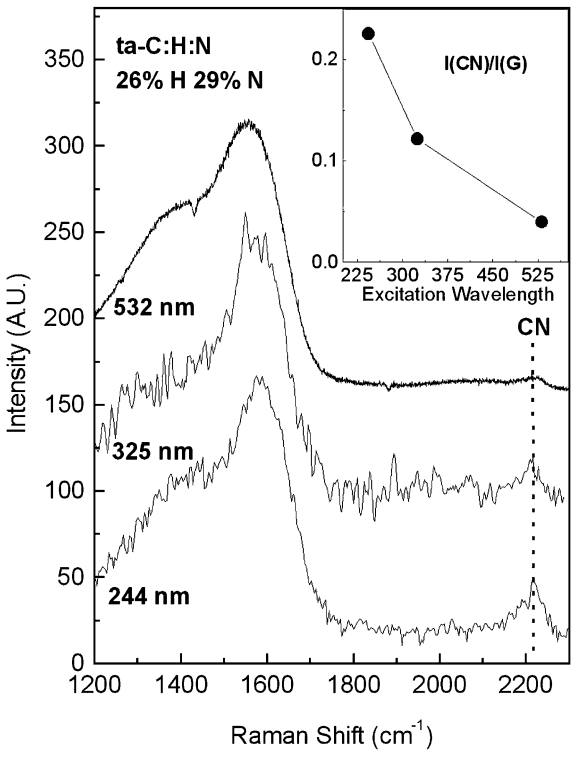

Fig. 3. Multi-wavelength Raman spectra of a ta-C:H:N film with ~26% H and 29% N, deposited by ECWR

514 nm excitation, whereas it falls sharply with N content for 244 nm excitation, from 1665 to 1590 cm^{-1}. This indicates that N addition has replaced the C=C olefinic groups with aromatic groups. The G peak position varies roughly linearly with excitation wavelength [4]. Fig. 2b plots the dispersion (slope) of the G peak wavenumber with excitation wavelength against the N content. The dispersion falls sharply up to 15% N, and then declines gradually until it reaches a constant value above 25% N.

sp^1 bonded −CN groups give rise to stretching modes approximately 2200 cm^{-1}. Fig. 1 shows that the 2200 cm^{-1} mode is clearly seen for 244 nm excitation, whilst it was barely detectable for 514 nm excitation. The mode's intensity increases by an order of magnitude, as the excitation changes from 514 to 244 nm, as shown in the insert. The enhancement of sp^1 C≡N groups in UV excitation occurs because this group has a $\pi-\pi^*$ band gap of 5–6 eV. The gap is relatively constant, it does not display the wide range of local gaps found for sp^2 bonded groups [3], so it is only resonant for UV excitation.

Figs. 3 and 4 show a similar set of data for a series of (t)a-C:H:N films deposited by a N_2/C_2H_2 plasma from an ECWR source [5]. The sp^3 content falls significantly above 20% nitrogen, and the gap rises, as the films become 'polymeric' [5]. Fig. 3 shows the multi-wavelength Raman spectra for a representative ta-C:H:N film. The variation of the G peak position is shown in Fig. 4. The G peak position decreases with N content for UV excitation from 1620 to 1600 cm^{-1}, and it goes up for visible excitation. These data are combined into the variation of G peak dispersion, and its variation with N content is shown in Fig. 4b. The dispersion falls almost linearly with N content. This shows that the sp^2 sites have become ordered in a more aromatic fashion for higher N contents, as discussed in more detail in Section III.

Fig. 3 shows the variation in the intensity of the C≡N sp^1 mode. The mode's intensity increases by an order of magnitude as the excitation changes from 514 to 244 nm, as shown in the insert, similar to that in (t)a-C:N, Fig. 1.

We finally consider a-C:N films prepared by magnetron sputtering at 200 °C with a deposition system as described by Wienss et al. [9]. Fig. 5a shows that variation of G peak for visible and UV excitation with N content. The G peak moves downwards in both cases, but now the fall for visible excitation is greater. Recall that in (t)a-C:N, the G peak was almost constant for visible excitation, Fig. 2a, whilst it moved up in (t)a-C:H:N, Fig. 4a. Fig. 5b shows the G peak dispersion

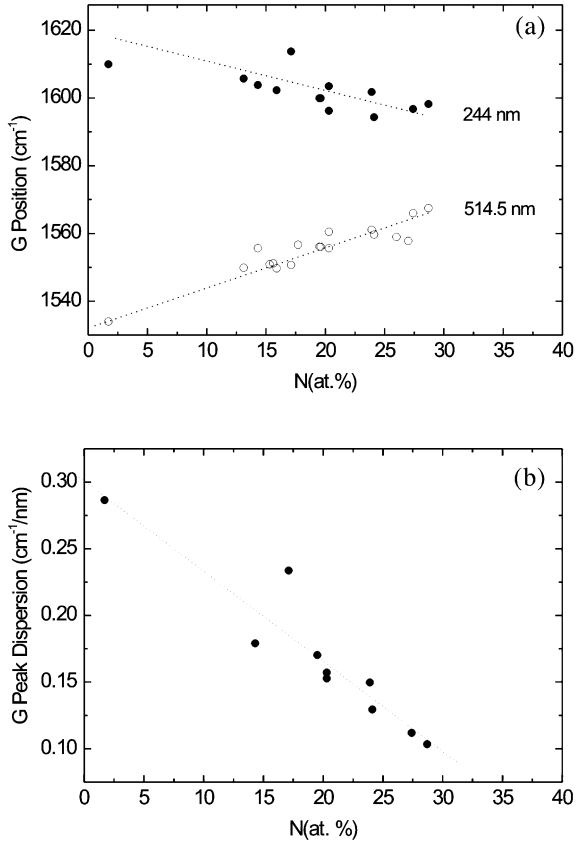

Fig. 4. (a) Variation of G peak position with N content at 244 and 514 nm excitation for (t)a-C:H:N films. (b) variation of G peak dispersion with N content. The lines are guides to the eye.

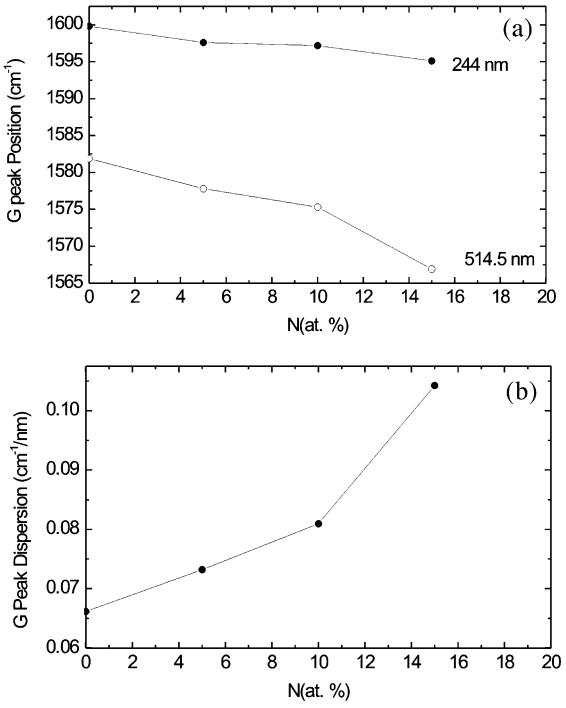

Fig. 5. (a) Variation of G peak position with N content for 244 and 514 nm excitation for high temperature deposited sputtered a-C:N films. (b) variation of G peak dispersion with N content.

against N content. The dispersion increases with N content, whereas for the previous (t)a-C:N and (t)a-C:H:N it decreased, Fig. 2b, Fig. 4b. The increase is because N is introducing disorder into the sp^2 sites, whereas in tetrahedral materials, N was inducing sp^2 ordering.

3. Interpretation of the raman spectra of carbon nitrides

We can thus now fully extend the three-stage model for multi-wavelength excitation [4] to explain the trends in the Raman parameters in any carbon nitride measured at any excitation wavelength. In particular, we will consider the trends in the G peak position, as summarised in Fig. 6.

We recall that, in general, adding N causes an independent evolution of the sp^3 fraction and sp^2 clustering. This causes a non-uniqueness of sp^2 configuration for a given sp^3 content [3,4]. This means that the ordering trajectory resulting by adding N to ta-C or ta-C:H is not equivalent to the reverse of the amorphization trajectory leading from a-C to ta-C. Thus, for a certain sp^3 content, we can have various G peak positions, both in visible and UV-excitation. Fig. 6 plots the schematic variation of G peak position for 244 and 514 nm excitations in carbon nitrides. The triangular shaped region representing the non-uniqueness for visible excitation becomes a 'bow-tie' shaped region for 244 nm, as defined in Fig. 6 [4]. The direction of the arrows indicates if we are following an amorphisation trajectory (from left to right, defined by the bold arrows in Fig. 6) or an ordering trajectory, from right to left (limited by the left-pointing continuous arrows in Fig. 6). The non-uniqueness regions are defined by the dotted, left-pointing arrows.

Fig. 6 immediately explains the trends for (t)a-C:N and (t)a-C:H:N. Clustering in UV Raman causes a G peak downshift with increasing N content for stage 3 carbons. As explained above, clustering means following the ordering trajectory in Fig. 6. The downshift is larger for higher initial G peak positions above 1600 cm^{-1}, the band limit for graphite. On the contrary, clustering raises the G peak for visible excitation. This upshift is larger the lower the initial G peak position. Thus, following the ordering trajectory, the G peak trends for UV and visible excitation are opposite for stage 3 carbons. This is what is seen in Fig. 2a and Fig. 4a, and is predicted by Fig. 6. Furthermore, this trend inversion, between visible and UV Raman, causes a G peak dispersion that is higher for lower sp^2 clustering, i.e. for lower N content in carbon nitrides. Again, this prediction

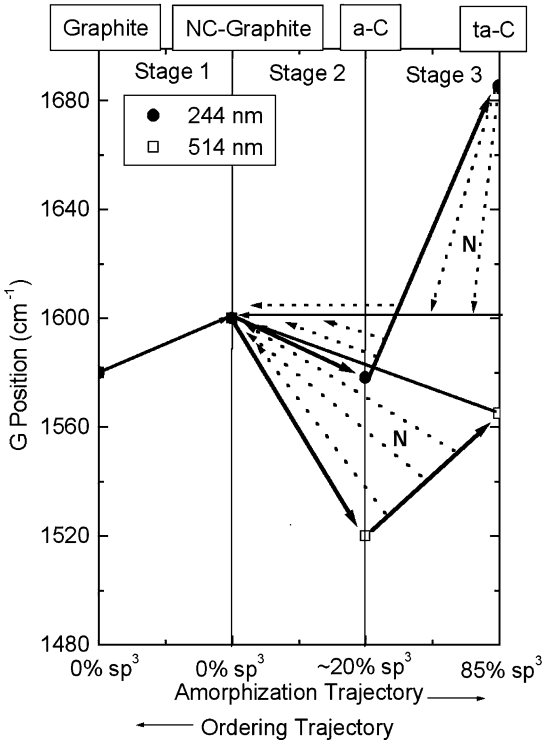

Fig. 6. Three stage model of the variation of the G peak position vs. disorder for visible and UV excitation in amorphous carbon nitrides. The bold right-pointing arrows represent the amorphisation trajectory is stages 2 and 3. The 'bow-tie' and trinagular-shaped regions defined by the dotted and continuous left-pointing arrows define the non-uniqueness regions for UV and visible excitations respectively. N introduction generally induces non-uniqueness in stage 3, as indicated by the letter N in the graph.

of Fig. 6 is seen experimentally in Fig. 2b and Fig. 4b. The G peak dispersion thus allows us to resolve the ambiguity that non-uniqueness can cause for single excitation energy measurements, especially in the visible, as seen, e.g. in Fig. 2a, where there is almost no variation of G peak position with N content at 514 nm. This implies that the G peak dispersion is the main parameter to be linked with N content, or sp^2 fraction, as indeed shown by its well-defined trends in Figs. 2 and 4.

It has been noted how nitrogen addition in a-C may increase its hardness and elastic recovery, especially at temperatures higher than 150 °C [6,9,23]. In that case, N does not cause more clustering of sp^2 sites, but a cross-linking [6,24]. We thus expect a relation between sp^3 content and sp^2 configuration with increasing N content, since the decrease of sp^2 clustering means that we are following the amorphization trajectory. This is the case of the sputtered carbon nitrides of Fig. 5. They can be classified as stage 2 carbons with increasing amorphisation. From Fig. 6, we see the amorphisation trajectory for stage 2 carbons predicts a decrease of G peak position for both visible and UV Raman spectra (bold right-pointing arrows). Fig. 6 also predicts a larger decrease for 514 nm excitation. This implies that the G peak dispersion must increase for increasing N content, as is indeed experimentally seen, Fig. 5b.

In general, we can also find cases were N induces clustering also in stage 2 carbons, e.g. for low temperature depositions. In this case, Fig. 6 predicts a rise of G position in the visible and also for UV excitation (dotted right-pointing arrows). There is no more the trend inversion typical of stage 3 carbons. However, the raise of G with N for UV excitation is lower than the corresponding raise for visible excitation, as shown in Fig. 6. Thus, even without trend inversion, this again results in a lower G peak dispersion with increasing N content. Thus for any carbon, a lower G peak dispersion always means ordering and vice-versa an increase of G peak dispersion always means disordering. This again shows that the G peak dispersion is the simplest, most direct way to characterise amorphous carbon nitride films in terms of N content, gap, sp^2 or sp^3 content, and, thus [25], hardness and density. This is demonstrated in the example outlined in Fig. 7. Fig. 7a plots the G-peak positions measured at 514.5 and 244 nm excitations for a series of carbon nitrides films deposited by sputtering and high current arc [26] as a function of the density. It is hard to see a coherent trend in Fig. 7a. If we now consider the G-peak dispersion and plot it against the density we get the clear trend of Fig. 7b. This shows again how the G peak dispersion is the parameter of choice for the characterisation of carbon nitride films.

Finally, we stress how Fig. 6 is not a fit to experimental data, but a predictive scheme, even if for clarity

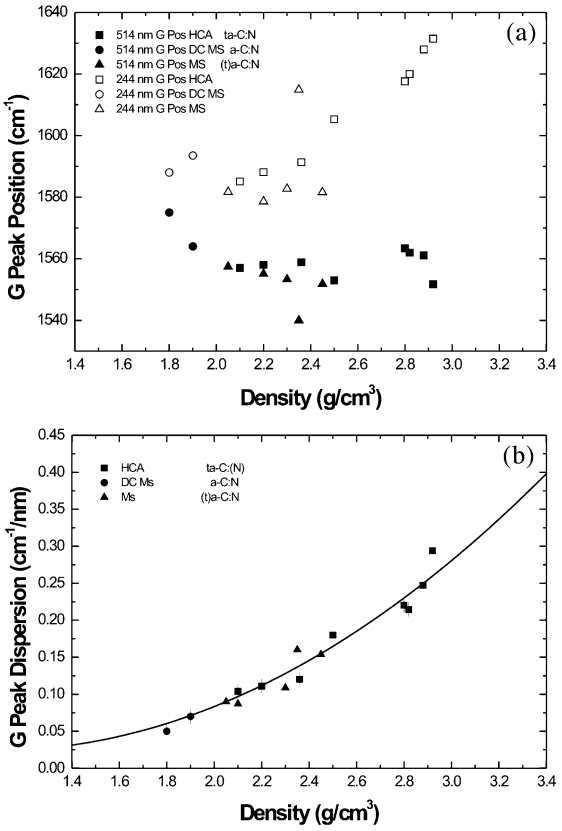

Fig. 7. (a) G peak position measured at 514 and 244 nm as function of the mass density for different carbon nitride films deposited by High Current Arc (HCA), Magnetron Sputtering (MS) and DC Magnetron Sputtering (DC MS) [25]. No clear trend can be identified. (b) G peak dispersion as function of the mass density. A clear correlation over a large density region is seen.

we introduced it as a summary of the results. Indeed it is derived form the general model of the G peak evolution in N-free samples [3,4]. It is the same as fig. 12 of ref. [4], having the non-uniqueness specified as induced by N rather than by other factors like annealing. Thus, all the experimental trends in this paper could predicted by Fig. 6. Indeed the increase of the G peak dispersion in high temperature sputtered a-C:N, where N induces disorder, is a most definitive proof that the three stage model works for carbon nitrides.

4. Conclusions

We classified amorphous carbon nitride films in four classes, according to the corresponding N-free film: a-C:N, a-C:H:N, ta-C:H:N and ta-C:N. We showed how the Raman spectra taken at any excitation energy can be explained in terms of an a-C based model, without need of extra peaks due to CN, NN or NH modes. The G peak dispersion emerges as a most informative parameter for Raman analysis. UV Raman enhances the sp^1

CN peak, which is usually too faint to be seen in visible excitation.

Acknowledgments

The authors thank D. Batchelder of University of Leeds, M. Stutzmann and M. Kuball of University of Bristol for the access to 244 and 325 nm Raman facilities. We thank M. Tommasini and C. Castiglioni for useful discussions, and M. von Gradowski, R. Ohr and H. Hilgers of IBM Mainz for sputtered CN samples. A.C.F. acknowledges Pembroke College and the Royal Society for financial support.

References

[1] A.Y. Liu, M.L. Cohen, Science 245 (1989) 841.
[2] S. Muhl, J.M. Mendez, Diamond Relat. Mater. 8 (1809) 1999.
[3] A.C. Ferrari, J. Robertson, Phys. Rev. B 61 (2000) 14095.
[4] A.C. Ferrari, J. Robertson, Phys. Rev. B 64 (2001) 075414.
[5] S.E. Rodil, A.C. Ferrari, J. Robertson, W.I. Milne, J. Appl. Phys. 89 (2001) 5425.
[6] N. Hellgren, M.P. Johansson, E. Broitman, L. Hultman, J.E. Sundgren, Phys. Rev. B 59 (1999) 5162.
[7] S.R.P. Silva, J. Robertson, G.A.J. Amaratunga, B. Rafferty, L.M. Brown, D.F. Franceschini, G. Mariotto, J. Appl. Phys. 81 (1997) 2626.
[8] J. Schwan, V. Batori, S. Ulrich, H. Ehrhardt, S.R.P. Silva, J. Appl. Phys. 84 (1998) 2071.
[9] A. Wienss, G. Persch-Schuy, R. Hartmann, P. Joeris, U. Hartmann, J, Vac. Sci. Technol. A 18 (2000) 2023.
[10] N.M. Victoria, P. Hammer, M.C. Dos Santos, P. Alvarez, Phys. Rev. B 61 (2000) 1083.
[11] M.C. Polo, J.L. Andujar, A. Hart, J. Robertson, W.I. Milne, Diamond Relat. Mater. 9 (2000) 663.
[12] G. Mariotto, F.L. Freire, C.A. Achete, Thin Solid Films 241 (1994) 255.
[13] (a) J.R. Shi, X. Shi, Z. Sun, S.P. Lau, B.K. Tay, H.S. Tan, Diamond Relat. Mater. 10 (2000) 76
(b) J.R. Shi, X. Shi, Z. Sun, S.P. Lau, B.K. Tay, H.S. Tan, Thin Solid Films 366 (2000) 169.
[14] Y.H. Chen, B.K. Tay, S.P. Lau, X. Shi, X.L. Qiao, J.G. Chen, Y.P. Wu, C.S. Xie, App. Phys. A 73 (2001) 341.
[15] Y.H. Cheng, B.K. Tay, S.P. Lau, X. Shi, X.L. Qiao, Z.H. Sun, J.G. Chen, Y.P. Wu, C.S. Xie, Diamond Relat. Mater 10 (2001) 2137.
[16] A.C. Ferrari, Diamond Relat. Mater. 11 (2002) 1053.
[17] M.R. Wixom, J. Am. Ceram. Soc. 73 (1973) 1990.
[18] A.K.M.S. Chowdhury, D.C. Cameron, M.S.J. Hashimi, Thin Solid Films 332 (1998) 62.
[19] M.K. Fung, W.C. Chan, Z.Q. Gao, I. Bello, S.T. Lee, Diamond Relat. Mater. 8 (1999) 472.
[20] Y.K. Yap, S. Kida, T. Aoyama, Y. Mori, T. Sasaki, Appl. Phys. Lett. 73 (1998) 915.
[21] F.R. Dollish, W.G. Fateley, F.F. Bentley, Characteristic Raman Frequencies of Organic Molecules, Wiley, New York, 1974.
[22] Physical Methods in Heterocycle Chemistry, ed. by A.R. Katkritzki, Academic Press, New York, Vol II (1963), Vol IV (1971).
[23] H. Sjostrom, L. Hultman, J.E. Sundgren, S.V. Hainsworth, T.F. Page, G.S.A.M. Theunissen, J. Vac. Sci. Technol. A14 (1996) 56.
[24] F. Weich, J. Widany, T. Frauenheim, Phys. Rev. Lett. 78 (1997) 3326.
[25] A.C. Ferrari, J. Robertson, M.G. Beghi, C.E. Bottani, R. Ferulano, R. Pastorelli, Appl. Phys. Lett. 75 (1893) 1999.
[26] M.V. Gradowski, A.C. Ferrari, R. Ohr, B. Jacoby, H. Hilgers, H.H. Schneider, H. Adrian, Surf. Coat. Technol. to be published (2003).